PHYSICAL REVIEW B VOLUME 16, NUMBER 7 1 OCTOBER 1977

Q factor and resonance amplitude of Josephson tunnel junctions

R. F. Broom and P. Wolf
IBM Zurich Research Laboratory, 8803 Rüschlikon, Switzerland
(Received 13 June 1977)

The surface impedance of the superconducting films comprising the electrodes of Josephson tunnel junctions has been derived from the BCS theory in the extreme London limit. Expressions have been obtained for (i) the dependence of the penetration depth λ on frequency and temperature, and (ii) the quality factor Q of the junction cavity, attributable to surface absorption in the electrodes. The effect of thin electrodes ($t \lesssim \lambda$) is also included in the calculations. Comparison of the calculated frequency dependence of λ with resonance measurements on Pb-alloy and all-Nb tunnel junctions yields quite good agreement indicating that the assumptions made in the theory are reasonable. Measurements of the (current) amplitude of the resonance peaks of the junctions have been compared with the values obtained from inclusion of the calculated Q in the theory by Kulik. In common with observations on microwave cavities by other workers, we find that a small residual conductivity must be added to the real part of the BCS value. With its inclusion, good agreement is found between calculation and experiment, within the range determined by the simplifying assumptions of Kulik's theory. From the results, we believe the calculation of Q to be reasonably accurate for the materials investigated. It is shown that the resonance amplitude of Josephson junctions can be calculated direct from the material constants and a knowledge of the residual conductivity.

I. INTRODUCTION

Self-induced peaks in the dc current of Josephson tunnel junctions, caused by coupling between the ac Josephson current and the standing-wave electromagnetic field in the cavity formed by the electrodes, are well known. These geometrical resonances were first observed by Fiske[1] and have since been studied both theoretically[2-7] and experimentally[2-5,8,9] to yield a fairly complete description of the mechanism. This, in turn, has made it possible to use the results obtained from resonance measurements to deduce a number of basic properties of tunnel junctions and of the superconductors from which they are made. Two examples are the determination of the capacitance of tunnel junctions[4,5,10] and the frequency and temperature variation of the penetration depth in the superconducting electrodes.[11-13] These quantities are determined by the *frequency* of the junction resonance, namely, the dc junction voltage. Rather less well documented, however, is the behavior of the *amplitude* of resonances. The most general theory of resonances is that by Kulik.[7] As in all theories, the cavity quality factor Q enters as an important parameter in determining the resonance amplitude. This contains several components corresponding to the various loss mechanisms in the cavity. Two of the most dominant are the surface losses in the electrodes, Q_e, and the dielectric loss due to the quasiparticle tunnel current, Q_d.

Previous measurements have consisted in measuring the resonance amplitude and then via the theory[7] estimating Q.[8,9] The results give evidence that the theory is qualitatively correct, but since Q is considered as a variable parameter, quantitative comparisons were not possible. We have carried out the reverse procedure of first calculating Q and then making direct comparisons between theory and the results obtained from measurements of the resonance amplitudes in Pb-alloy and Nb junctions. For this approach, the prime requirement was to calculate the surface impedance of the electrodes in order to obtain Q_e. The theory is based on the BCS description of electromagnetic effects as given by Matthis and Bardeen,[14] with the restriction that the films satisfy the condition for the local dirty limit, defined by a London penetration depth $\lambda \gg \xi_0/(1+\xi_0/l_N)$. This condition should be quite well fulfilled by our Pb-alloy and Nb junctions in which $l_N \lesssim 200$ Å.

The paper is divided into five sections. We summarize first, in Sec. II, the main results related to the surface impedance of the electrodes, in particular the cavity Q and the temperature and frequency dependence of the penetration depth. The latter is a useful check on the validity of the surface-impedance theory, and for this reason, we describe in Sec. III some experimental results on the frequency dependence of λ, obtained from resonance voltages. Section IV describes the experimental results on resonance amplitudes and their comparisons with the calculated Q values substituted in Kulik's theory.[7] The influence of varying the Josephson-current density j_1 (and hence the ratio L/λ_J where L is the junction length and λ_J the Josephson penetration depth) and the temperature for the two junction metallurgies Pb alloy and Nb is considered. Finally, in Sec. V we discuss the results and the range of validity of the theory.

II. THEORY

A. Thick electrodes, $t >> \lambda$

In view of the foregoing remarks concerning l_N it seems to be a reasonable approximation to use a formula for the surface impedance Z_S of the electrodes, which has been derived for the extreme London limit, $l_N = 0$, by Nam[15]:

$$Z_s = Z_{sn}(\sigma_1/\sigma_N + i\sigma_2/\sigma_n)^{-1/2} \tag{1}$$

in which Z_{sn} is the surface impedance in the normal state

$$Z_{sn} = (1+i)(\omega\mu_0/2\sigma_n)^{1/2} . \tag{2}$$

Combining Eqs. (1) and (2) and separating into real and imaginary parts yields

$$Z_s = R_s + iX_s = \left(\frac{\mu_0\omega}{2\sigma_n}\right)^{1/2} \frac{(\Sigma - \Sigma_2)^{1/2} + i(\Sigma + \Sigma_2)^{1/2}}{\Sigma} , \tag{3}$$

where σ_n is the normal-state conductivity, $\Sigma_1 = \sigma_1/\sigma_n$, $\Sigma_2 = \sigma_2/\sigma_n$, and $\Sigma^2 = \Sigma_1^2 + \Sigma_2^2$. The quantities σ_1/σ_n and σ_2/σ_n are the real and imaginary parts of the BCS normalized surface admittance. They were calculated numerically from expressions (3.9) and (3.10) of Ref. 14. Values appropriate to Pb and Nb at 4.2 °K are shown in Fig. 1. The abscissa is in units of reduced frequency $\Omega = \omega/\omega_g$, where $\omega_g = 2\Delta/\hbar$ with $2\Delta/e$ the gap voltage of the superconductor. It is important to note that in the case of the ac Josephson effect, the frequency $\omega = 2eV/\hbar$, hence for resonances at voltages V, the units are eV/Δ. At frequencies $\Omega < 1$, σ_1/σ_n is determined by the thermally excited quasiparticle density and is therefore strongly temperature dependent. At frequencies $\Omega \geq 1$ photons are absorbed by breaking of Cooper pairs, accounting for the sharp increase in σ_1/σ_n as Ω increases. In contrast, the imaginary part of the surface admittance σ_2/σ_n is nearly temperature independent over the whole frequency range at reduced temperature $T/T_c \leq 0.5$.

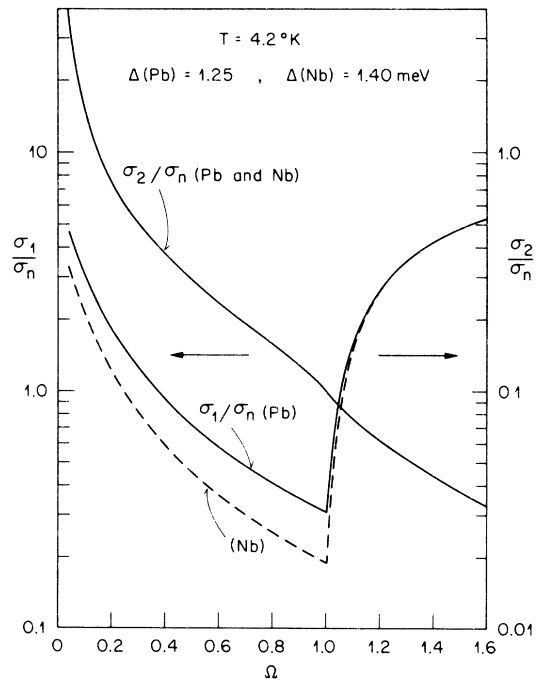

FIG. 1. Calculated values of the real (σ_1/σ_n) and imaginary (σ_2/σ_n) components of the normalized surface admittance for half-gap voltages $\Delta/e = 1.25$ and 1.4 mV, appropriate to Pb and Nb at 4.2 °K.

In the dirty limit at $T = 0, \omega = 0$, the penetration depth λ is[16]

$$\lambda = (2/\pi\omega_g\mu_0\sigma_n)^{1/2} , \tag{4}$$

and since $\lambda \equiv L/\mu_0$ and $X_S \equiv \omega L$ we can combine Eq. (4) with the imaginary part of Eq. (3) to yield

$$\frac{\lambda(\omega, T)}{\lambda(0,0)} = \frac{(\Sigma + \Sigma_2)^{1/2}}{\Sigma} \left(\frac{\pi\Delta(0)}{2\hbar\omega}\right)^{1/2} . \tag{5a}$$

Inspection of the values in Fig. 1 shows that $\sigma_2/\sigma_n \gg \sigma_1/\sigma_n$ for $\Omega \leq 1$, so in this region Eq. (5a) simplifies to

$$\frac{\lambda(\omega, T)}{\lambda(0,0)} = \left(\frac{\pi\Delta(0)}{\hbar\omega(\sigma_2/\sigma_n)}\right)^{1/2} . \tag{5b}$$

Thus the frequency and temperature variation can be calculated from σ_2/σ_n. The contribution of the electrodes to the junction quality factor Q_e is given simply by the ratio

$$Q_e = X_s/R_s = [(\Sigma + \Sigma_2)/(\Sigma - \Sigma_2)]^{1/2} . \tag{6a}$$

Again, when $\sigma_2/\sigma_n \gg \sigma_1/\sigma_n$, this simplifies to

$$Q_e = (2\sigma_2/\sigma_n)/(\sigma_1/\sigma_n) , \quad (Q_e > 5) . \tag{6b}$$

The full curves of Fig. 2 show Q_e calculated from Eq. (6a) for Pb and Nb at 4.2 °K. The dashed lines will be referred to later in Sec. IV.

At least one further contribution to the cavity Q must be considered, it is that caused by the quasiparticle tunnel current. The relation is

$$Q_d = \omega CR(V) = (2e/\hbar)\, VCR(V) \tag{7}$$

in which $R(V)$ is the voltage-dependent tunnel resistance, and C the capacitance of the junction.

Other contributions to Q such as dielectric loss and radiation from the junction we neglect on the grounds that they are not significant in comparison to Q_e and Q_d.[17] The combined Q from surface resistance and tunnel current is given by

$$1/Q_T = 1/Q_e + 1/Q_d . \tag{8}$$

It is relevant at this point to give a short summary of Kulik's results.[7] He finds that the ratio of the maximum current at resonance i_r to the dc Joseph-

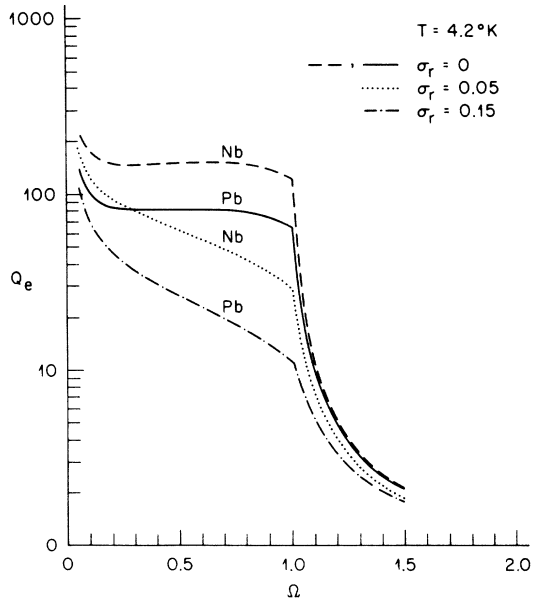

FIG. 2. Calculated Q_e as a function of normalized frequency Ω. The two upper curves are obtained from the data of Fig. 1, and the lower two with the inclusion of a residual conductivity σ_{res}, described in Sec. IV.

son current $i_1 (i_1 = j_1 A)$ is

$$i_r/i_1 = J_0(a) J_1(a) , \tag{9}$$

where J_0 and J_1 are the first two integer Bessel functions and a is given by the smallest root of the equation

$$2a = z J_0^2(a) \tag{10}$$

with

$$z = (L/\pi n \lambda_J)^2 Q_n , \tag{11a}$$

in which n is the mode number. When only the envelope of the resonant current maxima is required, it is convenient to rewrite Eq. (11a) as[18]

$$z = \frac{\hbar}{2e} \frac{j_1 Q(V)}{C_s V^2} , \tag{11b}$$

where C_s is the junction capacitance per unit area.

The solution of Eq. (10) yields a maximum in $i_r/i_1 = 0.34$ at $z = 4$,[19] and hence substituting the latter in Eq. (11b) yields a relation for the resonance voltage at which the resonance current has its maximum value, namely,

$$V(i_r = i_{r_{max}}) = \left(\frac{\hbar}{8e} \frac{j_1 Q(V)}{C_s} \right)^{1/2} . \tag{12}$$

B. Thin electrodes

In the dirty limit the surface impedance of a film of arbitrary thickness t is found to be

$$Z_s = (\mu_0 \omega / k) \coth(ikt) \tag{13}$$

with the wave number k,

$$k = (\tfrac{1}{2} \mu_0 \omega \sigma_n)^{1/2} [(\Sigma - \Sigma_2)^{1/2} - i(\Sigma + \Sigma_2)^{1/2}] . \tag{14}$$

Within the limits used in the approximation for the penetration depth $\lambda(\omega, T)$ in thick electrodes, Eq. (5b), we find for the penetration depth in thin electrodes $\lambda(\omega, T, t)$,

$$\lambda(\omega, T, t) = \lambda(\omega, T) \coth[t/\lambda(\omega, T)] . \tag{15}$$

With the same approximation, the following expression for $Q_e(t)$ is obtained:

$$Q_e(t) = \frac{Q_0 \sinh[2t/\lambda(\omega, T)] - \sin[2t/Q_0 \lambda(\omega, T)]}{\sinh[2t/\lambda(\omega, T)] + Q_0 \sin[2t/Q_0 \lambda(\omega, T)]} , \tag{16}$$

in which Q_0 is the value of Q_e for $t \gg \lambda(\omega, T)$.

The variation of $Q_e(t)/Q_0$ vs $t/\lambda(\omega, T)$ is plotted in Fig. 3. It decreases smoothly to the value of

TABLE I. Basic properties of the junctions used for resonance measurements. The last column indicates the figures in which data from the corresponding samples are given.

Sample No.	Material	T (°K)	$\Delta(T)$ (meV)	j_1 (A/cm^2)	i_1 (mA)	L/λ_J	Fig. No.
1	Pb alloy	4.16	1.25	1760	8.80	5.24	4
2	Pb alloy	5.34	1.09	535	2.675	2.85	7
3	Pb alloy	4.16	1.26	722	3.62	3.32	4, 7
4	Pb alloy	3.06	1.345	814	4.07	3.52	7
5	Pb alloy	1.90	1.36	840	4.20	3.58	7
6	Pb alloy	4.16	1.25	53	0.265	0.91	8
7	Pb alloy	4.16	1.25	1590	7.95	4.95	8
8	Nb-Nb	6.0	1.27	254	1.93	2.0	5
9	Nb-Nb	4.16	1.425	524	2.62	2.86	4, 5
10	Nb-Nb	3.14	1.44	558	2.79	2.95	5
11	Nb-Nb	1.95	1.45	578	2.89	3.01	5
12(2)	Nb-Nb	4.16	1.40	178	0.89	1.64	6
13(2)	Nb-Nb	4.16	1.40	1570	7.85	4.90	4, 6

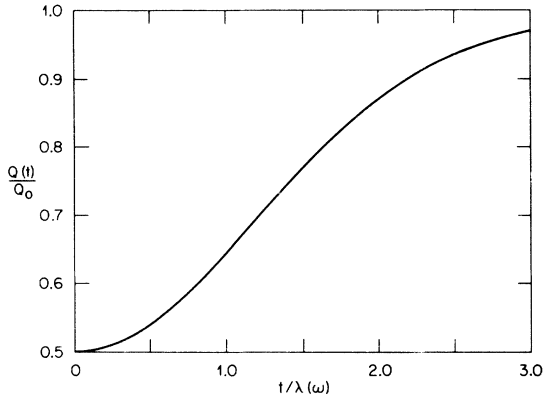

FIG. 3. The dependence of Q_e on normalized electrode thickness $t/\lambda(\omega)$, obtained from Eq. (16).

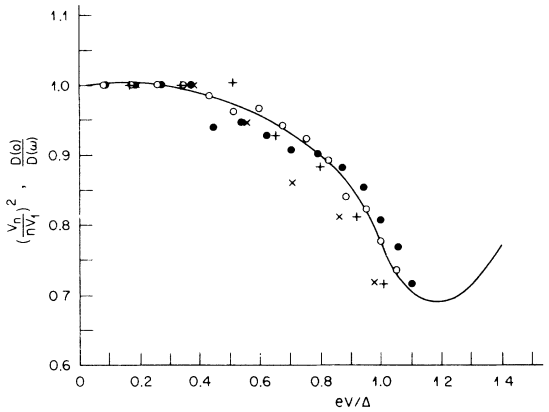

FIG. 4. Comparison of the experimental and calculated frequency dependence of the penetration depth of Nb and Pb at 4.2 °K. ○●, Nb junctions; +×, Pb-alloy junctions. Solid line calculated for Nb using the constants listed in Table II.

$\frac{1}{2}$, independent of Q_0, as $t/\lambda(\omega, T)$ approaches zero.

The Josephson tunnel junctions used for the investigations were all of the simple cross-line type of length $L = 50$ μm and $W = 10$ μm, deposited on oxidized Si substrates. The Pb-alloy junctions, containing In and Au,[20] were fabricated by a process similar to that first described by Greiner, Basavaiah, and Ames.[21] The tunnel barriers of the Nb junctions were likewise grown in an rf plasma of Ar and O_2 as described previously.[22] Some of the most important physical constants of the junctions are listed in Table I.

III. FREQUENCY DEPENDENCE OF λ

The resonance voltage V_n for the nth mode is given by[5]

$$V_n = \frac{nhc}{4eL}\left(\frac{\epsilon_0}{C_s d}\right)^{1/2}, \tag{17}$$

where ϵ_0 is the permittivity of free space and, for thick electrodes $(t \gg \lambda)$, $d = t_{ox} + \lambda_1 + \lambda_2$. Because λ_1 and λ_2 are not independent of frequency, the voltage steps $V_n - V_{n-1}$ are not equally spaced, but vary according to $[d(\omega_1)/d(\omega_n)]^{1/2}$ assuming that C_s is independent of frequency. Given $\lambda_{1,2}(0,0)$ and the electrode thicknesses, the latter ratio can be calculated from Eqs. (5) and (15) and compared with the experimental variation of $V_1, \ldots, V_n$. This has been reported for Sn,[11] Pb,[12] and Nb,[13] but, because it is important for the following section, we include some additional results for Pb and Nb in Fig. 4. Here the crosses are the measured values of $(V_n/nV_1)^2$ for two Pb junctions at 4.2 °K, while the circles are for two Nb junctions. The abscissa is in units of the half-gap voltage Δ/e.

The continuous curve is the calculated ratio $D(0)/D(\omega)$, where

$$D(\omega) = t_{ox} + \sum_{i=1}^{2} \lambda_i(\omega, T) \coth \frac{t_i}{\lambda_i(\omega, T)}, \tag{18}$$

based on the values of the parameters listed in Table II, and assuming $t_{ox} \sim 25$ Å. The values calculated for Pb and Nb are coincident to within ≤5% and so only a single curve is shown, that for Nb. Pb is a strong coupling superconductor, and Fulton and McCumber[23] have shown that σ_2/σ_n in the limit $\omega \to 0$ is reduced by the factor 0.788 compared to the BCS value. Nevertheless, Fig. 4 shows that the *relative* frequency dependence of σ_2/σ_n is not greatly different from the BCS values, although it is perhaps significant that the agreement between the Nb results and BCS is somewhat better.

IV. RESONANCE MEASUREMENTS

A. General considerations

The Josephson penetration depth λ_J appearing in Eq. (11a) is frequency dependent because it is

TABLE II. Parameters of Pb and Nb junctions used in the calculation of $D(\omega)$.

Material	Δ (meV)	$\lambda_1(0)$	$\lambda_2(0)$ (Å)	t_1	t_2 (Å)	V_1 (mV)
Pb alloy	1.25	1100	800	2000	3000	0.21 –0.24
Nb	1.40	880	880	1400	2500	0.125–0.13

proportional to $d^{-1/2}$, hence at high frequencies, the right-hand side of Eq. (11a) must be multiplied by the factor $d(\omega)/d(0)$ which can in turn be obtained from Eq. (5b). In comparing experiment with theory, Q_d was evaluated from the measured quasiparticle tunnel resistance at each resonant voltage, Eq. (7), and Q_e was calculated for the same voltages using the measured values of Δ and T. No correction was made either to Q_e or d for the influence of the finite electrode thickness. The smallest ratio t/λ occurs in the base electrode of the Nb junctions, leading to an overestimate in Q_e of about 11%, which is comparable to the uncertainties in other parameters, in particular $d(0)$ and i_1. For small values of the ratio $L/\lambda_J \leq 2$, j_1 was determined from the dc Josephson current i_m set to its maximum value i_1 by application of an external magnetic field in the plane of the junction and perpendicular to its length. For higher ratios, $L/\lambda_J \geq 2$, a correction for self-field effects, based on one-dimensional junction theory,[24,25] was made to obtain j_1. In all cases, the value of $i_1 \equiv j_1 A$ was used to determine the ratio i_r/i_1. The current i_r was obtained direct from the resonance current maximized by adjustment of the external magnetic field, less the corresponding quasiparticle tunnel current.

Low-order resonances in junctions having $L/\lambda_J > 2$ were difficult to measure; either they were lower in amplitude than the dc Josephson current at the appropriate magnetic field, or they were not stable in the sense that the junction voltage would only occasionally lock at the resonance voltage during the saw-tooth current waveform at 120 Hz used to display the I-V characteristics on an oscilloscope. Such cases were omitted from the data. Also, in the region of small mode number and $L/\lambda_J > 2$, the resonant amplitude was influenced by the direction of the external magnetic field. Higher amplitudes were generally observed with the external field in opposition to the self-field caused by the junction current, namely, in the direction of increasing dc Josephson current, rather than adding to the self-field. This is to be expected, since partial cancellation of the self-field leads to a more uniform current distribution within the junction. The former condition is indicated in the following Figs. 5–8 by open circles or rectangles. At higher mode numbers, the resonance amplitudes become independent of the direction of the external field, and results are indicated by closed symbols only.

At high voltages $V_n \geq \Delta/e$, the high damping through pair breaking causes the resonant modes to overlap and eventually merge into a continuum. Hence, in this range, measurements are inaccurate and tend to overestimate the amplitude of an individual resonance.

B. Niobium junctions

Figure 5 shows the measured values of i_r/i_1 versus normalized voltage eV/Δ for a Nb junction at several temperatures between 1.95 and 6 °K. The two dashed curves in Figs. 5(a) and 5(d) are the calculated envelopes of the resonance current, obtained from Eqs. (6a), (7), and (8) to yield Q_T,[26] and Eqs.(11a) and (5a) to calculate z and hence i_r/i_1 at each resonance voltage. It is evident that the agreement with experiment is quite good at 6 °K but very poor at 1.95 °K. In the latter case the value of the calculated Q_e is apparently much too high

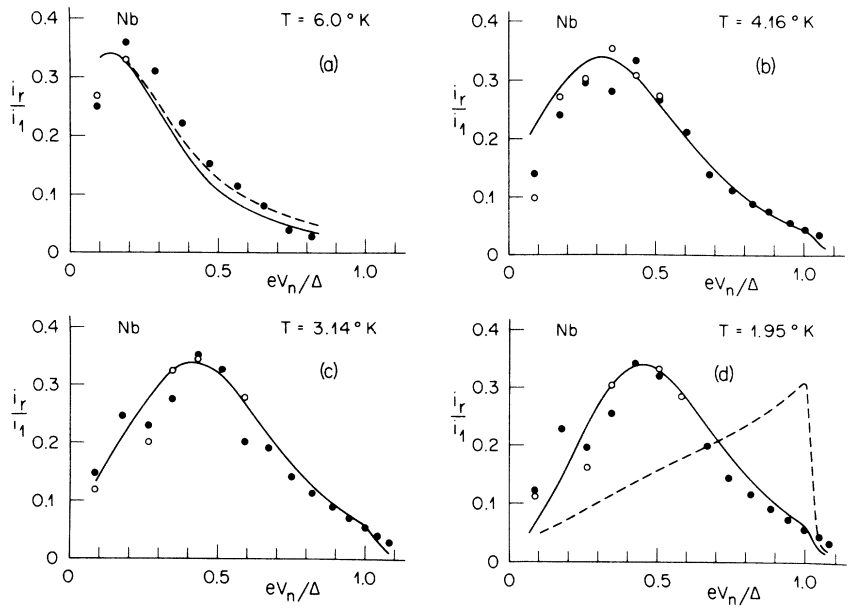

FIG. 5. Comparison of measured and calculated resonance current ratios i_r/i_1 for a Nb junction at four different temperatures: $T = 6$, 4.16, 3.14, and 1.95 °K. ○● experimental points, --- calculated using the BCS values of Q_e, — calculated with inclusion of $\sigma_{res} = 0.05$.

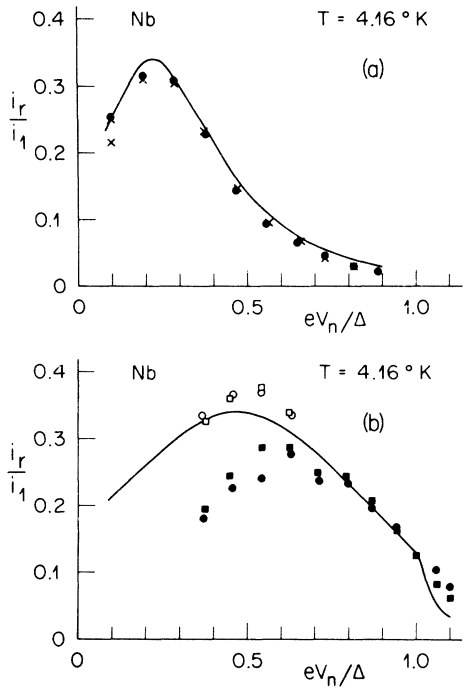

FIG. 6. Experimental and calculated values of i_r/i_1 for four Nb junctions at 4.16 °K. (a) $L/\lambda_J = 1.64$, (b) $L/\lambda_J = 4.9$. The calculated curves are obtained for $\sigma_{res} = 0.05$.

in comparison with experiment. Similar effects have been noted in most studies of superconducting resonant cavities,[27-29] where it is found that the real part of the surface impedance R_s tends experimentally to a constant value, the residual resistance R_{res} as the temperature is reduced. In the BCS formulation, $R_s \to 0$ as $T \to 0$. Several possible mechanisms have been proposed for the origin of R_{res}. They include surface imperfections[29] and phonon generation effects.[30] Assuming that the increase in the real part of the normalized conductivity is temperature and frequency independent, the influence on R_s and Q_e can be obtained by adding a constant σ_{res} to σ_1/σ_n.

The full curves of Fig. 5 are obtained with a value of $\sigma_{res} = 0.05$, chosen to yield the best overall agreement at all measured temperatures. This value of σ_{res} is about 10 times higher than that estimated from the data of Halbritter[29] for pure Nb cavities. Results for low and high current densities at 4.16 °K are shown in Fig. 6. As in Fig. 5 the curves are calculated with $\sigma_{res} = 0.05$. In the case of low j_1, ($L/\lambda_J \sim 1.64$) there is good agreement between the results for the two samples and the calculated curve over the whole range. However, for the two high-current-density samples it was not possible to measure the three lowest-order modes and there is a considerable difference between the points for the external field parallel and antiparallel to the self-field. As noted previously, the latter have greater amplitude than the former. Nevertheless, the maximum in the ration i_r/i_1, as in the other curves, does not deviate greatly from the theoretical value of 0.34 and at high orders n the agreement with calculated values is quite fair. In all other Nb junctions studied, but not reported here, the resonant amplitudes could be fitted without changing σ_{res} from its value of 0.05. This is consistent with the observation that the tunneling characteristics were all very similar, showing only small deviations from one another, apart from the current scaling factor.

C. Pb-alloy junctions

In the case of Pb-alloy junctions, a higher value of $\sigma_{res} = 0.1-0.15$ was required to obtain a fit between theory and experiment. Figures 7 and 8 show, respectively, the temperature variation of i_r/i_1 and results for two junctions having widely different current densities. The curves of Fig. 7 are calculated with $\sigma_{res} = 0.15$, while those of Figs. 8(a) and 8(b) are with $\sigma_{res} = 0.12$ and 0.10, respectively. All results are qualitatively similar to those for Nb, the principal differences being the wider separation of the resonance modes (because of the lower capacitance C_s) and the larger σ_{res} of the former.

To investigate whether the relatively high σ_{res} in the Pb-alloy junctions could be caused by free Au or $AuPb_3$,[31] in the counter-electrodes two sets of junctions were prepared in which one set had no Au in the top film and the other 4 wt. %. In both cases, σ_{res} was 0.11 ± 0.01. In the latter case, σ_{res} was also unchanged after annealing the junctions for 1 h at 80 °C. In view of this result, it is unlikely that the Au in either electrode has much influence on σ_{res}, leaving as remaining possibilities either the approximate 10-wt. % In in solution with the Pb of the base electrode, or the Pb itself. Which of these is the major contribution is not clear at present.

The calculated values of Q_e including σ_{res} are indicated in Fig. 2 by the two lower curves. For Nb, $\sigma_{res} = 0.05$ and for Pb, $\sigma_{res} = 0.15$ were used in the calculation. As noted in the previous section, the low-frequency value of σ_2/σ_n for Pb is lower than the BCS value, and the results of Fig. 4 suggest that this factor is not reduced at frequences within $0 \leq \hbar\omega \leq \Delta$. Assuming that σ_2/σ_n retains its BCS value within this range, the greatest reduction in Q which we can expect is by the strong coupling factor 0.788. When this is applied to the calculated Q_e, σ_{res} has to be correspondingly reduced by approximately the same factor, 21%, which does not

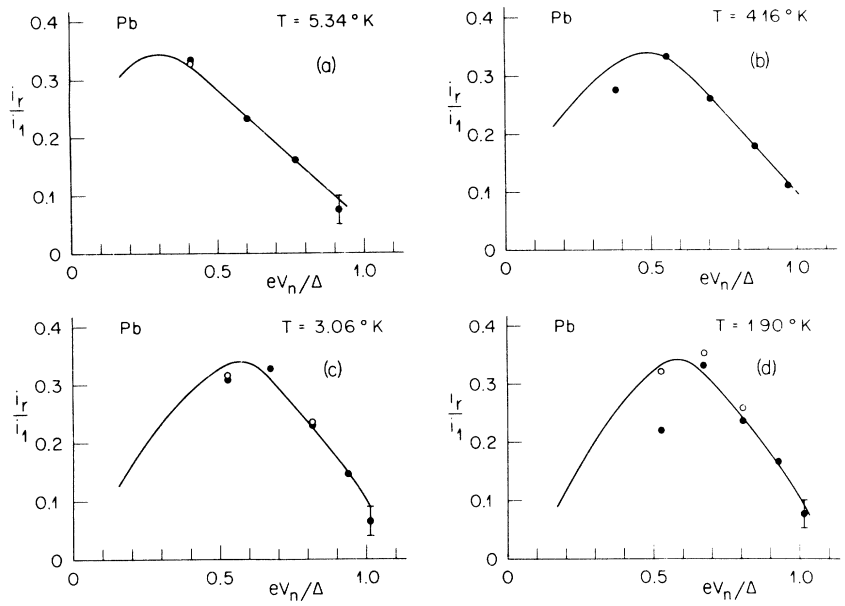

FIG. 7. As Fig. 5 but for a Pb-alloy junction and calculated curves obtained with $\sigma_{res} = 0.15$.

greatly alter the situation.

However, it must be noted that the fitted values of σ_{res} for both Nb and Pb are likely to be somewhat high as they embody all losses not accounted for separately, such as dielectric loss in the junction oxide, coupling of radiation out of the cavity, and especially the reduction in Q caused by the finite electrode thickness.

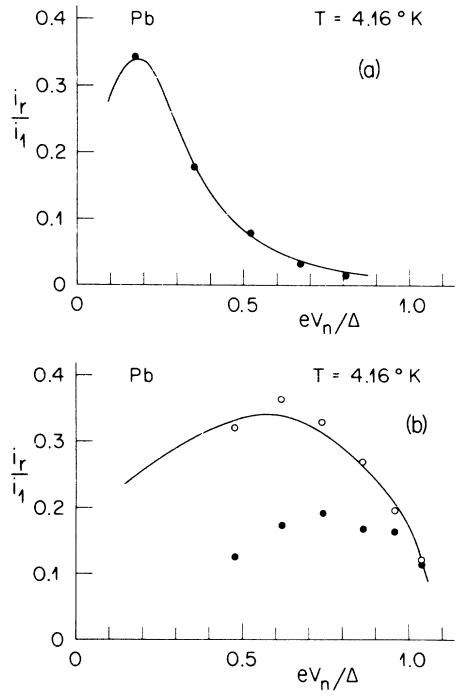

FIG. 8. Pb-alloy junctions at $T = 4.16$ °K. (a) $L/\lambda_J = 0.91$. (b) $L/\lambda_J = 4.95$. The calculated curves are obtained with $\sigma_{res} = 0.12$ and 0.1 in (a) and (b), respectively.

V. SUMMARY

Studies of the temperature and frequency dependence of the penetration depth in Nb,[13] together with the results shown in Fig. 4, indicate fair agreement with the BCS description, as applied in the dirty limit. Although Pb and Pb-In alloys are strong coupling superconductors to which the BCS theory does not strictly apply, the data of Fig. 4 indicate that the *variation* of $\lambda(\omega)$ follows the BCS theory reasonably well. In addition, measurements on a Nb-NbO_x-Pb junction show that the temperature dependence of $\lambda(0, T)$, obtained from measurements of the dc Josephson current minima with applied field, is also in good agreement with BCS.

In view of these results, it is reasonable to assume that the calculation of the surface losses in the electrodes (Q_e) is fairly accurate. The necessity of including a residual conductivity in the calculations, although outside the realm of basic theory, is nevertheless in qualitative agreement with nearly all previous findings in studies of superconducting microwave cavities. Accepting that the calculated values of Q are not seriously in error, we can now draw some conclusions regarding the range of validity of Kulik's theory,[7] based on the results shown in Figs. 5–8:

(i) The maximum resonance current amplitude $i_r/i_1 = 0.34$ predicted by theory appears to be true in all cases within the limits of experimental error, providing self-field effects are corrected for in obtaining i_1. This is in agreement with re-

sults reported by Gou and Gayley.[8]

(ii) For $L/\lambda_J \leq 2$, theory and experiment are in good agreeement for all resonance voltages. This is consistent with the basic assumption of the theory that the self-field caused by the junction current has a negligible influence on the relative phase distribution along the junction.

(iii) For $L/\lambda_J > 2$, three voltage ranges can be identified: (a) At low voltages, below that yielding the maximum resonance amplitude $V(i_{r\ max})$ as defined by Eq. (12), theory and experiment do not agree. (b) In the region of $V(i_{r\ max})$ there is fair agreement provided the external field is applied in a direction antiparallel to the self-field of the junction. This yields higher resonance currents than when the external field adds to the self-field of the junction. (c) At higher voltages, up to and above Δ/e, and correspondingly higher external fields there are many flux quanta in the junction, resulting in a *mean* current distribution which is fairly uniform. In this case, agreement is again quite good for both directions of external field.

The calculated values of Q_e, shown in Fig. 2, decrease very abruptly when the resonance voltage $V_n > \Delta/e$, ($\hbar\omega > 2\Delta$), due to pair breaking. Experimentally, the abrupt change in slope is not observed because the gap voltage is distributed over 50–100 μV. Nevertheless, all samples show a strong decrease in resonance amplitude and considerable broadening of the linewidth as V_n exceeds Δ/e. Although quantitative measurements cannot easily be made in this region owing to overlapping of the modes, the results are qualitatively in agreement with theory.

ACKNOWLEDGMENTS

Thanks are due to U. Deutsch, W. Heuberger, and W. Walter for their important contribution in the preparation of the Josephson junctions.

[1]M. D. Fiske, Rev. Mod. Phys. 36, 221 (1964).
[2]R. E. Eck, D. J. Scalapino, and B. N. Taylor, Phys. Rev. Lett. 13, 15 (1964).
[3]R. E. Eck, D. J. Scalapino, and B. N. Taylor, in *Proceedings LT9, Columbus, Ohio*, 1964, edited by J. G. Daunt, D. O. Edwards, F. J. Milford, and M. Yaqub (Plenum, New York, 1965), p. 415.
[4]I. M. Dmitrenko, I. K. Yanson, and V. M. Svistunov, Zh. Eksp. Teor. Fiz. Pis. Red. 2, 17 (1965) [JETP-Lett. 2, 10 (1965)].
[5]D. N. Langenberg, D. J. Scalapino, and B. N. Taylor, Proc. IEEE 54, 560 (1966).
[6]I. O. Kulik, Zh. Eksp. Teor. Fiz. Pis. Red. 2, 134 (1965) [JETP-Lett. 2, 84 (1965)].
[7]I. O. Kulik, Zh. Tekh. Fiz. 37, 157 (1967) [Sov. Phys.-Tech. Phys. 12, 111 (1967)].
[8]Y. S. Gou and R. I. Gayley, Phys. Rev. B 10, 4584 (1974).
[9]K. Schwidtal and C. F. Smiley, in *Proceedings LT13, Boulder, Colorado, 1972*, edited by K. D. Timmerhaus, W. J. O'Sullivan and E. F. Hammel (Plenum, New York, 1974), Vol. 4, p. 575.
[10]K. Schwidtal, J. Appl. Phys. 43, 202 (1972).
[11]J. Matisoo, J. Appl. Phys. 40, 2091 (1969).
[12]G. E. Peabody and R. Meservey, Phys. Rev. B 6, 2579 (1972).
[13]R. F. Broom, J. Appl. Phys. 47, 5432 (1976).
[14]D. C. Mattis and J. Bardeen, Phys. Rev. 111, 412 (1958).
[15]S. B. Nam, Phys. Rev. 156, 487 (1967).
[16]This is obtained by comparing the BCS equations in Ref. 14 with the corresponding equations for the two-fluid model. It can also be obtained from the relation $\lambda = \lambda_L(\xi_0/l_N)^{1/2}$ for dirty alloys.
[17]N. F. Pedersen, T. F. Finnegan, and D. N. Langenberg, Phys. Rev. B 6, 4151 (1972).
[18]Obtained by writing z in terms of the wave velocity $\bar{c}$ and then substituting the definitions for $\bar{c}$ and λ_J.
[19]A further factor $F_n(H)$ on the right-hand sides of Eqs. (8) and (9) is here set equal to unity. It is only significant for $n = 1$ and 2, where it is 1.09 and 1.03, respectively.
[20]S. K. Lahiri, J. Vac. Sci. Technol. 13, 148 (1976).
[21]J. H. Greiner, S. Basavaiah, and I. Ames, J. Vac. Sci. Technol. 11, 81 (1974).
[22]R. F. Broom, R. Jaggi, R. B. Laibowitz, and W. Walter, in *Proceedings LT14, Otaniemi, Finland*, 1975, edited by M. Krusius and M. Vourio (North-Holland, Amsterdam, 1975), Vol. 4, p. 172.
[23]T. A. Fulton and D. E. McCumber, Phys. Rev. 175, 585 (1968).
[24]C. S. Owen and D. J. Scalapino, Phys. Rev. 164, 538 (1967).
[25]S. Basavaiah and R. F. Broom, IEEE Trans. Magnetics, MAG-11, 759 (1975).
[26]In calculating Q_d from Eq. (7) a constant value of $C = 10$ and 4 μF/cm^2 for Nb- and Pb-alloy junctions, respectively, was used in this and all subsequent calculations.
[27]J. P. Turneaure and I. Weissman, J. Appl. Phys. 39, 4417 (1968).
[28]Y. Bruynserade, O. Gorle, D. Leroy, and P. Morignot, Physica (Utr.) 54, 137 (1971).
[29]J. Halbritter, J. Appl. Phys. 42, 82 (1971).
[30]E. Kartheuser and S. Rodriguez, J. Appl. Phys. 47, 700 (1976).
[31]S. Basavaiah and S. K. Lahiri, J. Appl. Phys. 45, 2773 (1974).